SAND--88-3033

DE91 006745

Distribution
Category UC-814

SAND88-3033
Unlimited Release
Printed November 1990

Two-dimensional Velocity Models for Paths from Pahute Mesa and Yucca Flat to Yucca Mountain*

Marianne C. Walck

Geophysics Division

James S. Phillips

Ground Motion and Seismic Division

Sandia National Laboratories
Albuquerque, New Mexico 87185

ABSTRACT

Vertical acceleration recordings of 21 underground nuclear explosions recorded at stations at Yucca Mountain provide the data for development of three two-dimensional crystal velocity profiles for portions of the Nevada Test Site. Paths from Area 19, Area 20 (both Pahute Mesa), and Yucca Flat to Yucca Mountain have been modeled using asymptotic ray theory travel time and synthetic seismogram techniques. Significant travel time differences exist between the Yucca Flat and Pahute Mesa source areas; relative amplitude patterns at Yucca Mountain also shift with changing source azimuth. The three models, UNEPM1, UNEPM2, and UNEYF1, successfully predict the travel time and amplitude data for all three paths.

Quality Level of Work Performed

This work was performed at a Quality Assurance Level of I.

Acknowledgments

The team for the Weapons Test Seismic Investigations Project collected and processed the ground motion data presented in this report. J. G. Lee, J. D. Pearcey, J. W. Long, and K. A. Sabisch all contributed to the completion of this study through data acquisition and processing.

Contents

Preface

The Yucca Mountain Project, managed by the Nevada Operations Office of the U.S. Department of Energy, is examining the feasibility of siting a repository for commercial, high level nuclear wastes at Yucca Mountain, on and adjacent to, the Nevada Test Site. This work, intended to extend our understanding of the ground motion at Yucca Mountain resulting from testing of nuclear weapons on the Nevada Test Site, was funded by the Yucca Mountain project and the Military Applications Weapons Test Program. PDM 75-8, Analysis of ground motion data in support of the quantification of seismic risk of the Yucca Mountain site, is the associated Problem Definition Memo. This report summarizes one aspect of the weapons test seismic investigations conducted in FY1988.

List of Tables

List of Figures

1 Introduction

Understanding the risks associated with the effects of strong ground motions from seismic events on a geologic repository is important for evaluation of the Yucca Mountain proposed nuclear waste storage site. The Yucca Mountain Project is conducting studies to help quantify the expected ground motion levels from seismic sources that may occur during the repository lifetime. Both natural (earthquake) and artificial (explosion) sources of seismic energy must be considered. Nuclear tests conducted at the nearby Nevada Test Site (NTS) comprise the largest source of artificially produced seismic energy observed at Yucca Mountain. Ground motions from these underground nuclear explosions have been monitored at Yucca Mountain since 1980 by the Weapons Test Seismic Investigations Project at Sandia National Laboratories. Several types of analyses of these triaxial ground motion data have been undertaken, including observations of vector peak motions (Vortman, 1985), observations of individual component peak motions, analysis of attenuation of ground motion as a function of sensor depth (Vortman and Long, 1982a,b), and prediction of pseudo relative velocity spectra at Yucca Mountain.

Ground motions result from the combined effects of source radiation, travel path characteristics, and receiver structure at the recording site. The amount of seismic energy radiated from an explosion depends on the yield and the coupling efficiency of seismic energy into the ground at the shot point. Absolute ground motion levels necessarily depend on the size of the explosion. Relative amplitude patterns, however, are fairly stable for groups of sources in small geographic areas and can be used to extract information about path and receiver effects. Receiver effects at Yucca Mountain remain to be documented in detail; studies using nuclear explosions as sources are currently underway. In this study, we assume similar source characteristics among groups of NTS tests and focus instead on the propagation path characteristics. Here we examine the two-dimensional velocity structure for three distinct routes from the NTS testing areas to Yucca Mountain. The source areas include two portions of Pahute Mesa (Area 19 and Area 20) and Yucca Flat (Figure 1). A total of 90 records from 21 nuclear explosions recorded at nine Yucca Mountain stations were analyzed to develop reasonable two-dimensional velocity models for the three paths. We used two-dimensional travel time and synthetic seismogram modeling procedures that are standard techniques in refraction seismology; these methods were developed by Červený et al. (1977) and McMechan and Mooney (1980). Our results demonstrate that reasonable models based on known geological and seismological information can accurately predict travel times and relative amplitudes of Pahute Mesa and Yucca Flat explosions recorded at Yucca Mountain. The information gained from modeling the explosion waveforms over travel path lengths of 37 to 57 km yields useful information about crustal velocities at depths

from the surface to about 8 km.

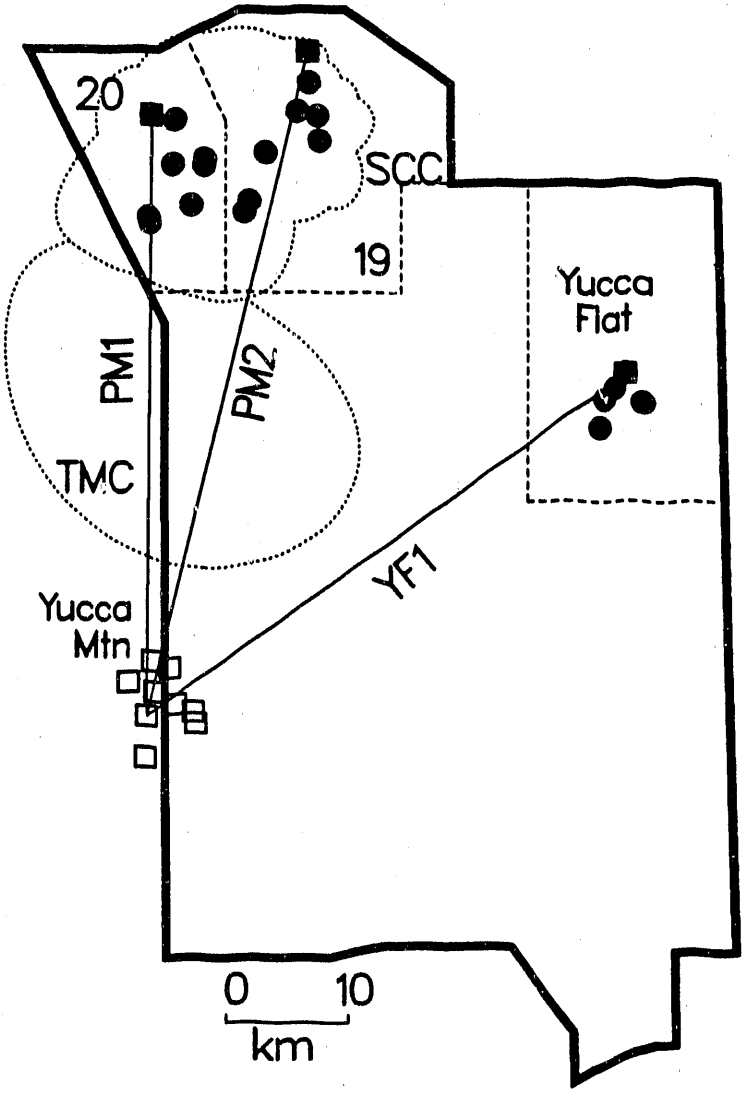

Figure 1: Location map showing Nevada Test Site, Yucca Mountain seismic stations (open squares), explosion locations (solid symbols), and velocity profiles PM1, PM2, and YF1. Also denoted are the Timber Mountain Caldera (TMC) and the Silent Canyon Caldera (SCC). Areas 19 and 20 comprise Pahute Mesa.

2 Data

In order to construct estimates of two-dimensional velocity structures between the nuclear testing areas and Yucca Mountain, we examined records of 21 different tests occurring in three portions of NTS (Areas 20, 19, and Yucca Flat). Table 1 lists the event locations; they are displayed in Figure 1. We grouped the 21 events into three general travel paths (Figures 1 and 2) designated PM1, PM2, and YF1. Paths PM1 (Area 20) and PM2 (Area 19) are represented by eight events each; there are five Yucca Flat tests providing data for the YF1 path. The final column in Table 1 shows the travel path assigned for each event. Table 2 contains the location data for the nine Yucca Mountain stations at which the ground motion data were recorded. Only surface recordings were used in this study; no downhole information was included.

The data used in the analysis are 90 vertical acceleration recordings from the 21 events (Table 3). The travel path distance ranges from 37 to 57 km for Pahute Mesa events and from 41 to 51 km for the Yucca Flat tests. Source-receiver azimuths range from 231° to 241° for the YF1 path, 177° to 190° for PM1, and 188° to 197° for the PM2 path. Recorded travel times vary from 7.43 to 10.83 seconds for Pahute Mesa shots and from 7.52 to 9.14 seconds for the Yucca Flat events. Figure 3 presents travel times for the three data groups, and Figures 4 and 5 display representative vertical acceleration seismograms, grouped by source, for the three different source areas.

The Pahute Mesa ground motion data recorded at Yucca Mountain differ substantially from the corresponding Yucca Flat data. Both the travel times and the relative amplitude patterns change significantly as a function of azimuth. In Figure 3, we display the travel time of the first arriving P wave as a function of distance for all three source areas. The data in Figure 3 demonstrate that over the entire distance interval, energy from Yucca Flat shots arrives earlier than energy from Pahute Mesa events at the same range. Within the Pahute Mesa data, there is a slight tendency for Area 19 travel times (Pahute Mesa 2) to be less than Area 20 times (Pahute Mesa 1). Also, the Yucca Flat travel times seem to have somewhat more scatter than the Pahute Mesa data. The large travel time discrepancy between Pahute Mesa and Yucca Flat of over 0.5 second indicates that major azimuthal differences exist in the shallow crustal velocity structure on the NTS. The faster Yucca Flat travel times are indicative of a YF1 travel path with generally higher velocities than PM1 or PM2. Drill hole logs from the Yucca Flat area indicate the presence of Paleozoic sedimentary rocks at extremely shallow depths (600 - 900 m). These rocks are represented in Yucca Flat velocity models with velocities reaching 5.9 km/s within 2 km depth (e.g., Harkrider, 1987). The early arrival times of Yucca Flat tests at Yucca Mountain are consistent with a travel path almost entirely in rocks with fast 'basement' velocities of about 5.9-6.0 km/s. In

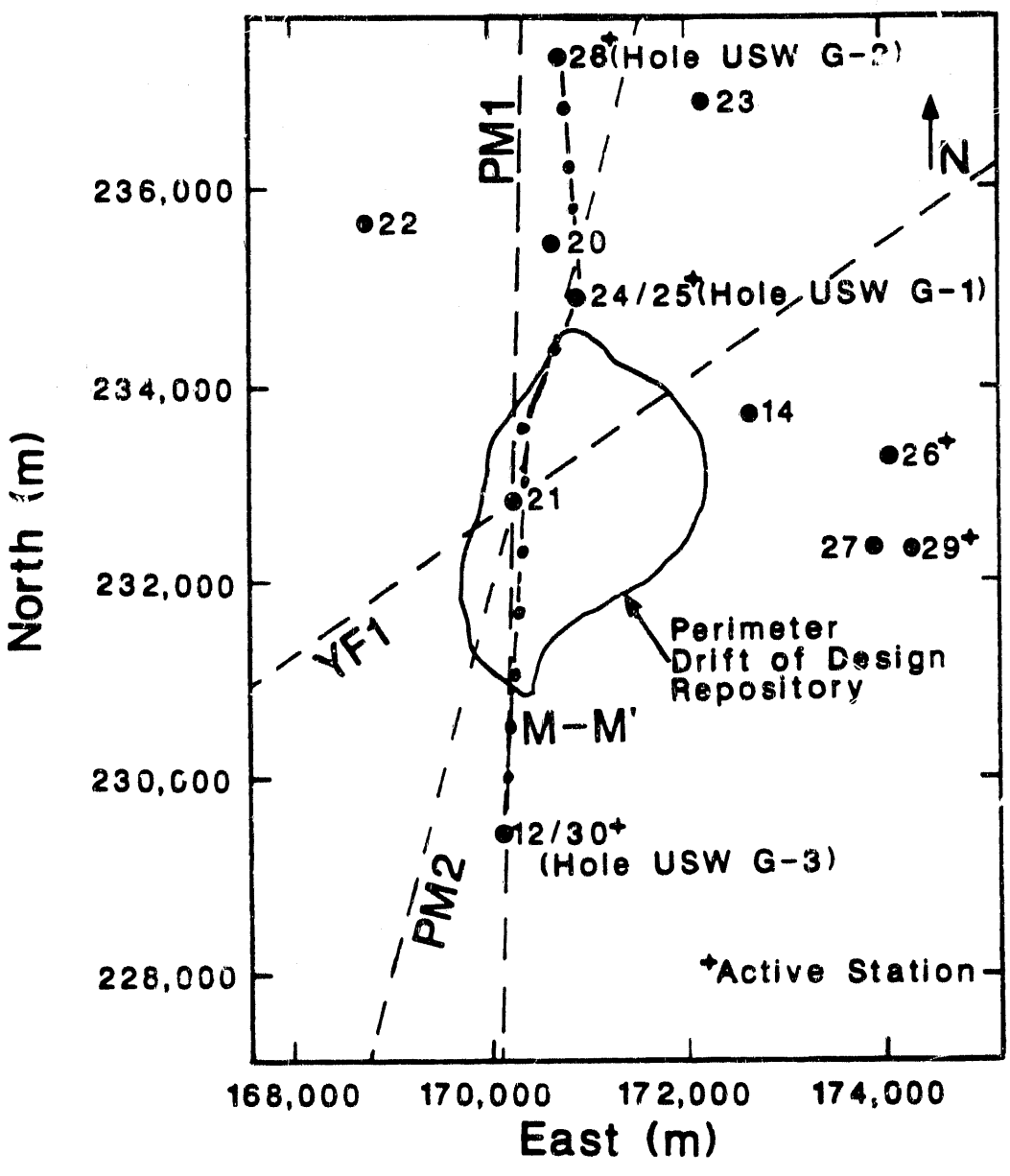

Figure 2: Close-up view of the Yucca Mountain area, showing accelerometer stations (dots), profiles (dashed lines) and cross-section M-M' of Ortiz et al. (1985) (dash-dot line).

Table 1: Event Location Data

Test Name	Nevada Coordinates North (m)	East (m)	GZ Elevation (m)	Depth of Burial (m)	Profile
Atrisco	259,169	211,090	1,295	640	YF1
Baseball	259,466	207,961	1,259	564	YF1
Belmont	274,078	170,596	1,900	605	PM1
Bodie	278,831	175,017	2,018	635	PM1
Cabra	283,007	170,719	1,934	543	PM1
Chancellor	279,934	180,038	2,040	625	PM2
Hardin	275,509	174,011	1,951	625	PM1
Harzer	283,343	182,636	2,100	637	PM2
Hermosa	260,329	208,788	1,278	640	YF1
Hosta	288,293	183,460	2,102	640	PM2
Jefferson	278,955	172,487	1,981	609	PM1
Kappeli	279,365	175,108	2,010	640	PM1
Labquark	282,981	184,248	2,100	616	PM2
Lockney	274,961	178,308	2,012	616	PM2
Molbo	274,534	170,505	1,900	638	PM1
Mundo	261,602	209,665	1,292	567	YF1
Nebbiolo	275,875	178,708	2,065	640	PM2
Serena	282,631	172,667	1,971	597	PM1
Serpa	285,720	183,551	2,055	573	PM2
Tierra	280,904	184,435	2,145	640	PM2
Tortugas	257,099	207,569	1,243	640	YF1

Table 2: Yucca Mountain Station Data

Station	Nevada Coordinates		Elevation
	North (m)	East (m)	(m)
14	233,834.22	172,741.17	1,255.40
21	232,863.74	170,350.47	1,482.18
22	235,645.59	168,888.02	1,579.81
23	236,852.46	172,250.29	1,447.28
24/25	234,842.25	170,992.11	1,325.46
26	233,233.42	174,163.06	1,111.00
28	237,286.85	170,846.62	1,553.87
29	232,288.84	174,365.15	1,108.56
30	229,421.89	170,231.54	1,480.20

contrast, several studies document Pahute Mesa velocities that are significantly slower than 6 km/s from the surface to depths of at least 4 km (Hartzell et al., 1983; Helmberger and Hadley, 1981; Taylor, 1983; Stump and Johnson, 1984). Thus the initial portion of the travel path from Pahute Mesa to Yucca Mountain is much slower than the corresponding section of the path from Yucca Flat to Yucca Mountain. This difference in the velocity structures of the source regions probably accounts for most of the observed travel-time disparity for the paths.

Patterns of observed first-arrival relative amplitudes for the Yucca Mountain stations are also quite different for the two source areas. General waveform characteristics are similar, with relatively small, long-period first pulses followed by a large,'ringy', high-frequency coda. The peak-to-peak relative amplitudes of the initial arrivals are quite consistent from event to event for both Yucca Flat and Pahute Mesa events. Figure 4 shows the initial waveforms for Atrisco and Hermosa, both Yucca Flat tests. The relative amplitudes between stations are correct as shown. For all of the Yucca Flat events studied, the stations to the east of Yucca Mountain (14 and 26) consistently exhibit the largest amplitudes. Stations 25, 22, and 30 record the smallest first arrival sizes. Stations with intermediate amplitudes include 23 and 21. These amplitude patterns are not the result of amplitude decay with increasing distance but reflect the combined effects of receiver and path structure.

Relative amplitude patterns for Pahute Mesa events are distinctly different from the

Table 3: Ground Motion Records Used in the Study

Test Name	Station	Distance (km)	Azimuth (deg)	Raw Travel Time (s)
Atrisco	23	44.801	240.1	8.00
	14	45.965	236.6	8.22
	24	46.905	238.8	8.35
	22	48.324	240.9	8.68
	21	48.501	237.2	8.67
Baseball	23	42.048	237.7	7.70
	14	43.345	234.0	7.85
	22	45.540	238.6	8.33
	21	45.854	234.7	8.29
Belmont	28	36.692	179.6	7.43
	25	39.237	179.4	7.87
	30	44.658	180.5	8.73
Bodie	28	41.654	185.8	8.32
	30	49.641	185.5	9.56
Cabra	23	46.180	178.1	9.105
	24	48.166	179.7	9.44
	14	49.215	177.6	9.52
	21	50.145	180.4	9.83
	30	53.588	180.5	10.29
Chancellor	23	43.780	190.3	8.63
	25	45.990	191.3	8.975
	21	48.057	191.6	9.38
	30	51.455	191.0	9.85
Hardin	28	38.254	184.7	7.74
	25	40.779	184.2	8.16
	30	46.244	184.7	9.01
Harzer	23	47.636	192.6	9.31
	22	49.639	196.1	9.73
	14	50.488	191.3	9.625
	21	51.953	193.7	10.01

Table 3
Ground Motion Records used in the Study
continued

Test Name	Station	Distance (km)	Azimuth (deg)	Raw Travel Time (s)
Hermosa	23	43.438	237.3	7.82
	26	43.969	232.0	7.88
	28	44.347	238.7	7.84
	29	44.401	230.8	7.93
	14	44.741	233.7	7.99
	25	45.588	236.0	8.13
	22	46.973	238.3	8.46
	21	47.250	234.4	8.46
	30	49.423	231.3	8.72
Hosta	23	52.647	192.3	10.115
	22	54.627	195.5	10.49
	14	55.504	191.1	10.455
	21	56.958	193.3	10.83
Jefferson	28	41.600	182.3	8.40
	25	44.131	181.9	8.82
	30	49.584	182.6	9.66
Kappeli	28	42.194	185.8	8.475
	23	42.609	183.9	8.55
	25	44.713	185.3	8.85
	21	46.744	185.8	9.29
	30	50.181	185.6	9.58
Labquark	28	47.522	196.4	9.33
	25	49.930	195.4	9.63
	30	55.362	194.7	10.43
Lockney	28	38.309	191.2	7.77
	30	46.249	190.1	9.00
Molbo	23	37.723	177.4	7.60
	22	38.923	182.4	7.85
	14	40.761	176.9	8.035
	21	41.671	180.2	8.335

Table 3
Ground Motion Records used in the Study
concluded

Test Name	Station	Distance (km)	Azimuth (deg)	Raw Travel Time (s)
Mundo	23	44.862	236.5	8.23
	26	45.445	231.4	8.28
	14	46.201	233.1	8.43
	25	47.026	235.3	8.55
	22	48.341	236.7	8.86
	21	48.701	233.8	8.95
	30	50.900	230.8	9.14
Nebbiolo	23	39.553	189.4	7.90
	22	41.410	193.7	8.29
	14	42.462	188.1	8.29
	21	43.815	191.0	8.66
Serena	28	45.281	182.3	9.03
	23	45.780	180.5	8.99
	22	47.138	184.6	9.27
	25	47.818	182.0	9.45
	21	49.821	182.7	9.73
	30	53.265	182.6	10.18
Serpa	22	52.178	196.3	10.105
	14	53.001	191.8	10.025
	21	54.480	194.0	10.41
Tierra	28	45.590	197.3	8.88
	14	48.502	194.0	9.24
	21	50.063	196.3	9.62
	30	53.406	195.4	10.09
Tortugas	23	40.719	240.2	7.52
	14	41.889	236.3	7.67
	25	42.818	238.7	7.86
	22	44.243	241.0	8.18
	21	44.423	236.9	8.15
	30	46.485	233.5	8.35

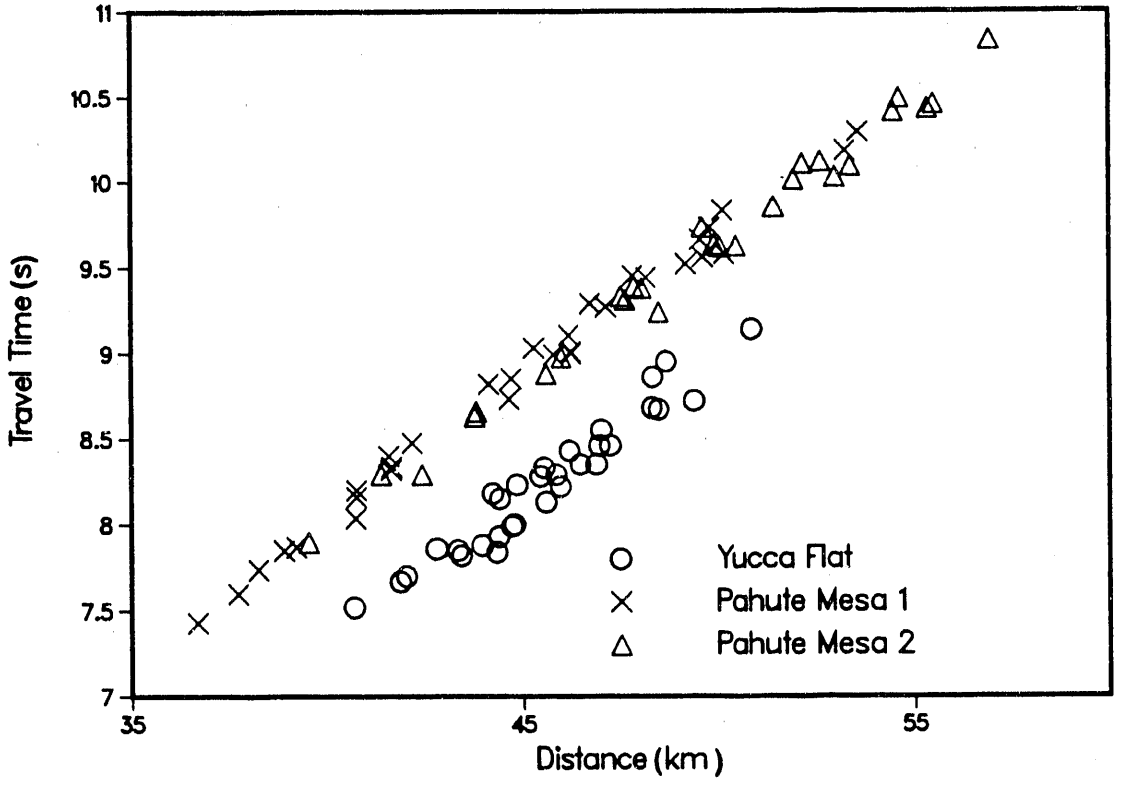

Figure 3: Travel time as a function of distance for nuclear tests recorded at Yucca Mountain.

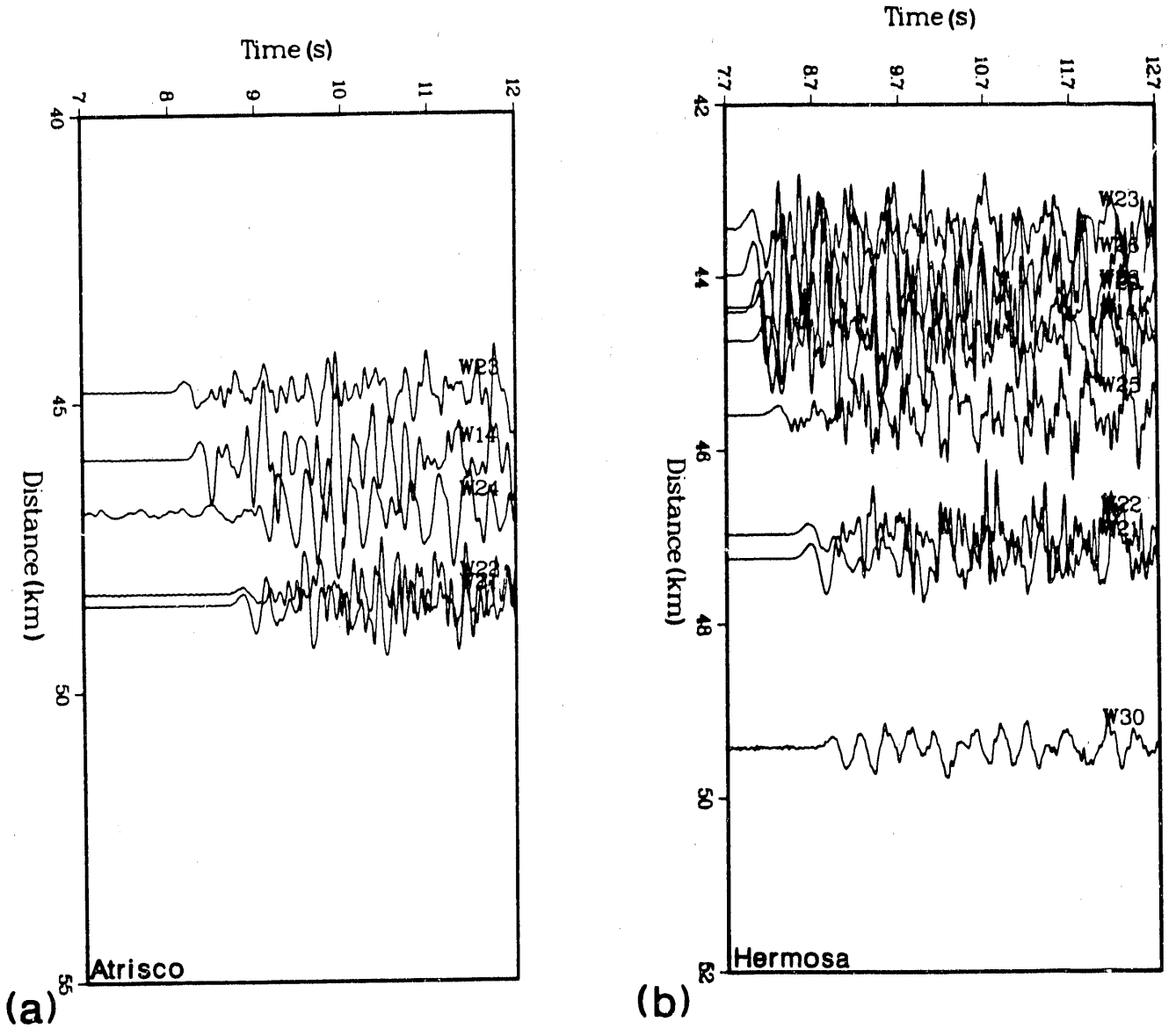

Figure 4: Acceleration waveforms as a function of distance for two Yucca Flat tests, Atrisco (a) and Hermosa (b). Note the large first-arrival amplitudes for stations 14, 16, and 29, and the smaller amplitudes for stations 22, 24, 25, and 30.

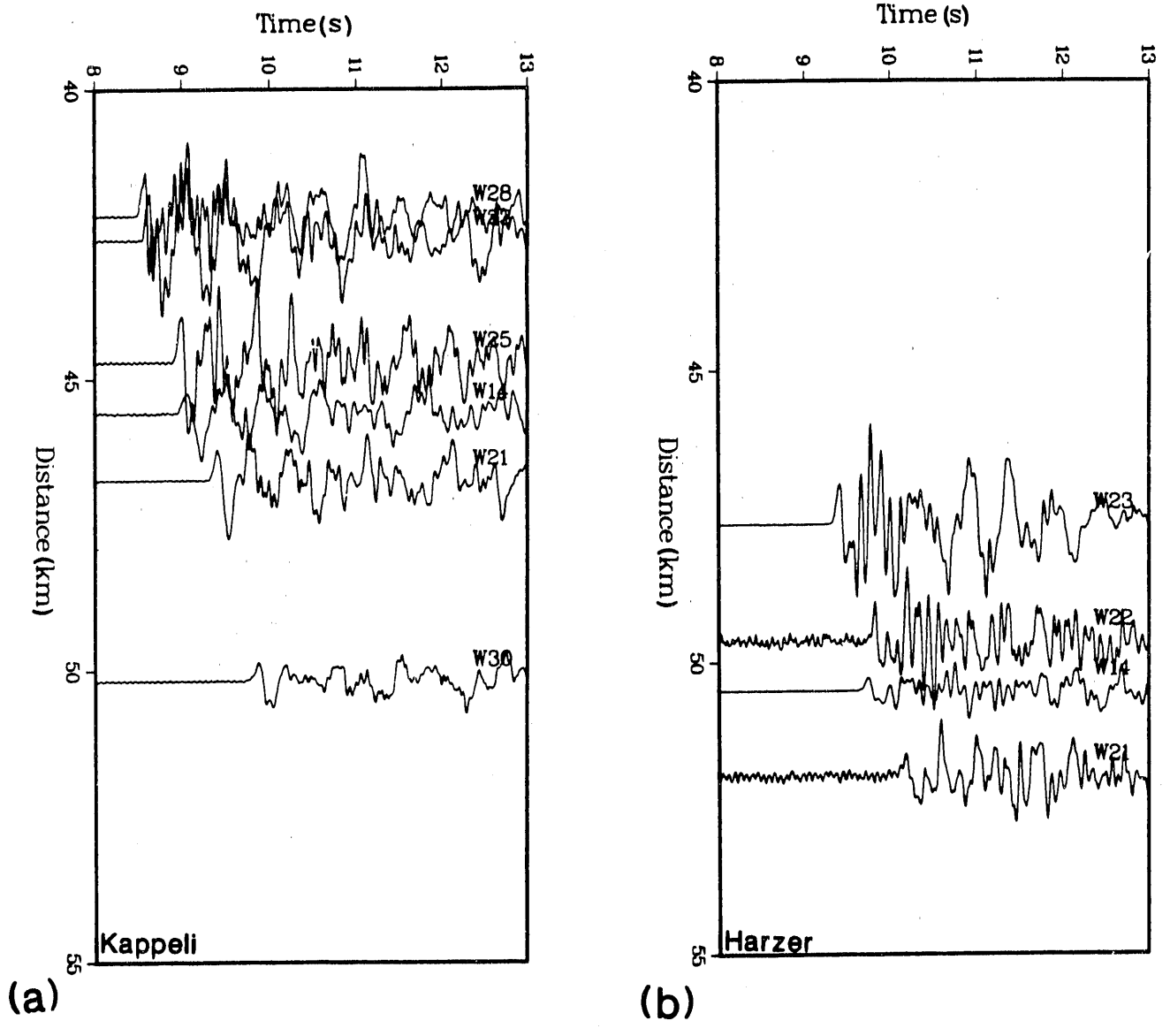

Figure 5: Acceleration waveforms as a function of distance for two Pahute Mesa tests, Kappeli (a) and Harzer (b). Kappeli represents the PM1 profile, amd Harzer the PM2 profile. Notice the large amplitudes associated with stations 28, 23, and 25, and the smaller first arrivals at stations 14 and 30.

pattern observed for Yucca Flat explosions. Station 14 no longer records relatively large amplitudes; now it consistently has lower amplitudes than most of the other stations. The largest amplitudes are seen at stations at the north end (28, 23, and 25) with the eastern stations (26, 29, and 14) being the smallest. Accelerations at station 22 are usually intermediate in size, while stations 21 and 30 display considerable variability in relative amplitude for Pahute Mesa events. Figure 5 contains representative record sections for Pahute Mesa events. The azimuthal variation of the relative amplitude patterns indicates that causative velocity variations are most likely not located directly beneath the stations, but lie elsewhere along the path. In Section 4, we will discuss velocity models that satisfy both the travel time and relative amplitude patterns for each path.

3 Analysis Method

The goal of this study is to derive models of the velocities within Earth's crust along the three travel paths shown in Figure 1. The distances between the sources and receivers place the analysis in the realm of refraction seismology. If a horizontally homogeneous, vertically layered velocity structure is assumed, it is simple to calculate the velocities needed to fit the travel times from a single source using standard refraction equations (e.g., Telford et al., 1976). If the layers dip, the profile must be reversed in order to determine the correct dip and velocities. Simple dipping layers, however, are rarely sufficient to provide realistic approximations to geologic structures in complex areas such as southern Nevada.

One method that allows modeling of travel times for more complex media, which vary in two dimensions, is called asymptotic ray theory (Červený et al., 1977). Asymptotic ray theory (ART) is an approximate method that is valid for computing travel times for seismic waves through structures varying both laterally and in depth, with some restrictions. For ART to be correct, the medium must change slowly with respect to the wavelength of the seismic waves to be modeled. Also, head waves are not included in the form of ART used here (zero-order) but are easily approximated using small velocity gradients below each layer boundary. ART has proven to be a versatile and extremely useful tool for modeling of seismic refraction data (Hill et al., 1985; Mooney and Colburn, 1985). It is considered a standard method in refraction seismology at the present time. Červený et al. (1977) wrote the computer program that implements the method; it traces rays through two-dimensional media. The appendix contains documentation of the code.

McMechan and Mooney (1980) extended ART to include calculation of realistic synthetic seismograms for media varying in two dimensions. A complex amplitude is calculated for each ray from the initial amplitude, geometrical spreading, and the product of the complex reflection and transmission coefficients along the path. To construct a synthetic seismogram for a given distance, rays must be traced that include all arrivals of interest covering the receiver distance range. The complex amplitude of the two closest rays for each phase are interpolated to produce the amplitude of the synthetic medium response at each phase arrival time. A source function (e.g., a Ricker wavelet) is then convolved with the amplitude response to produce the synthetic seismogram. Examples of use of the McMechan and Mooney (1980) algorithm are found in the work of Meltzer et al. (1987), Colburn and Mooney (1986), and Blumling et al. (1985). The accuracy of the ART synthetics is limited by restrictions inherent in the theory and because only the two closest rays are used to calculate the complex amplitude at any point in the model. A more rigorous method valid for two-dimensional structures, such

as finite differences (e.g., Vidale and Helmberger, 1988), would produce complete seismograms that have more accurate amplitudes than ART. The computational efficiency of ART, however, is a tremendous advantage in the iterative forward modeling process used to derive reasonable velocity models.

Our implementation of the ART procedure, including both travel time and synthetic seismogram calculations, is contained in RAY84 and R83PLT, a two-program package obtained from J. Luetgert of the U.S. Geological Survey. These versions of the Červený et al. (1977) and McMechan and Mooney (1980) codes have been used extensively (e.g., Hill et al., 1985; Klemperer and Luetgert, 1987; Valdes et al., 1986) and can be considered reliable. The appendix contains a more detailed discussion of these codes.

3.1 Modeling Procedure

The first step in deriving a velocity model for a profile is to match the model-predicted travel times to the observed data. Travel times are sensitive to the integrated velocity along the raypath from the source to the receiver; it is essential to model them correctly. After travel times are fit, we attempt to model the relative amplitude patterns recorded at the receivers, which are more sensitive to velocity gradients along the travel path. A model which satisfies, within reasonable limits, both travel time and relative amplitude data for a suite of sources is considered to be satisfactory. Because of the laterally varying velocity structure and our limited distribution of sources and receivers, we cannot derive unique models for the three profiles considered in this report. Other models could be derived which also satisfy the data.

Figure 6 displays the travel-time modeling procedure. The analyst constructs an initial model based on the available geologic and seismologic information. Rays are then traced through the model for a given source. Topography is included in the ray tracing code, so elevation corrections generally are not necessary. Next, we compare the model travel times to the actual times. If they do not match within a preselected criterion (here 0.075 s), then the analyst determines an adjustment to the model which may result in improved travel times, and traces the rays through the adjusted model. Several iterations of ray tracing and model adjustments may be required to obtain agreement between observed and model-generated travel times. After a satisfactory fit for one event is found, we go on to another source, located at a different point along the model, and continue. If the model must be changed to accommodate the times from subsequent events, we must return to the previous events and ascertain whether the new model generates acceptable travel times for those events. When a single model provides acceptable travel times for all receivers and all sources for a given profile, the final model is declared to be successful.

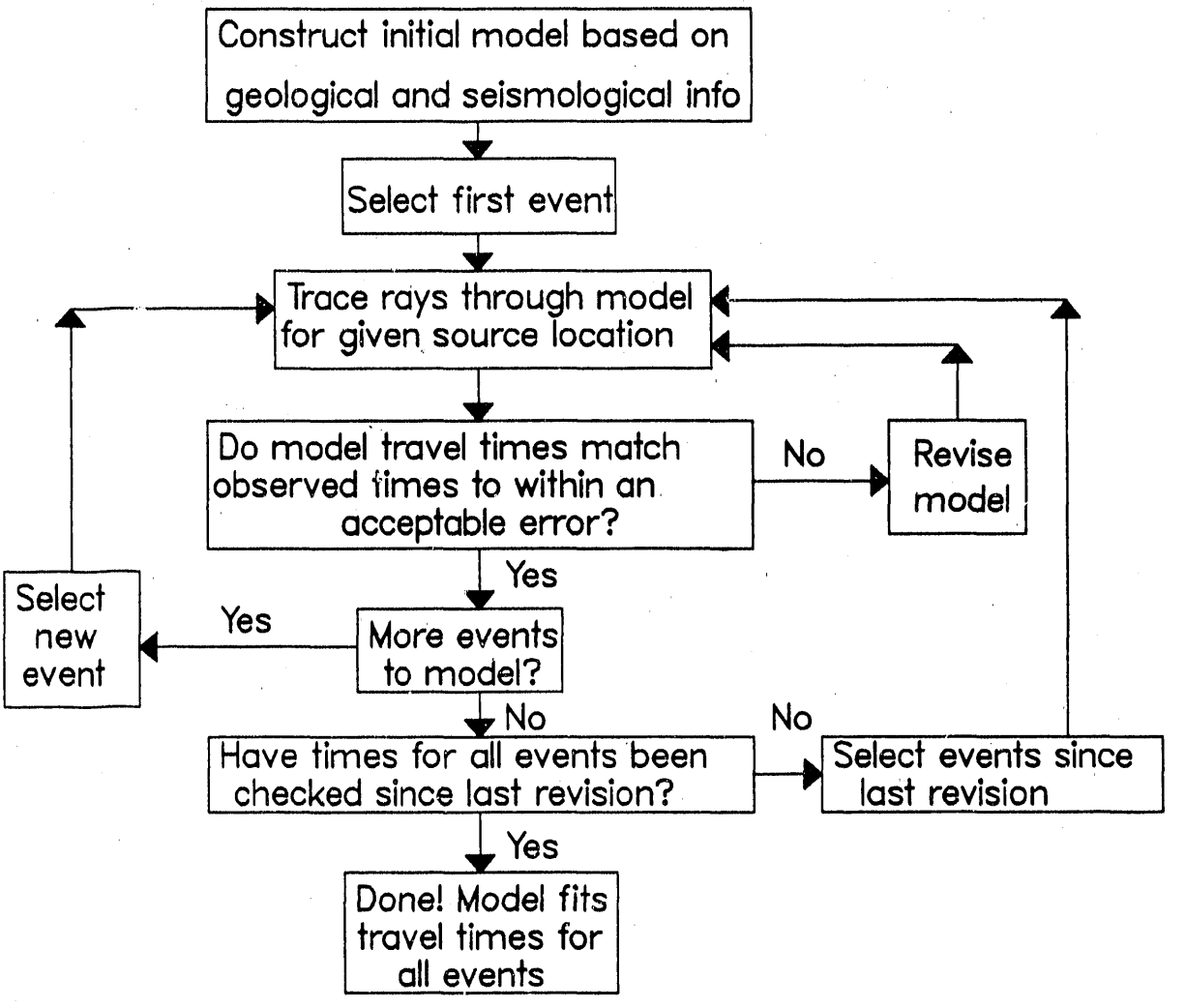

Figure 6: Flow chart of procedure used in modeling travel times.

Next, the travel-time model is used to generate synthetic seismograms for stations at the appropriate distances along the profile. If the relative amplitude patterns qualitatively match the data, this model is accepted. Otherwise, the model must be adjusted further until both travel times and relative amplitudes are satisfactory. The next section describes the application of this modeling procedure to the NTS explosion data recorded at Yucca Mountain.